Effects of Rare-Gas Matrices on the Optical Response of Silver Nanoclusters

R. Schira, Franck Rabilloud

Effects of Rare-Gas Matrices on the Optical Response of Silver Nanoclusters

Romain SCHIRA and Franck RABILLOUD*

Univ Lyon, Université Claude Bernard Lyon 1, CNRS, Institut Lumière Matière, F-69622, Villeurbanne, France

Corresponding author: franck.rabilloud@univ-lyon1.fr

Abstract:

The optical response of silver clusters, Ag_n with n = 8, 20, 35, 58, 92, embedded in a rare-gas matrix are calculated in the framework of the Time-Dependent Density Functional Theory (TDDFT). We present a methodology able to reproduce with unprecedented accuracy the experimental spectra measured on metal clusters embedded in neon, argon, krypton and xenon solid matrices. In our approach, the metal cluster is surrounded by explicit rare-gas atoms and embedded in a polarizable continuum medium. Interactions with the surrounding medium affects both the position and the width of the surface plasmon absorption band of metal clusters. The size dependent shift of the surface plasmon band is evaluated in the case of a neon matrix. While the band shifts to lower energies (red shift) for large clusters, it shifts to higher energies (blue shift) for very small clusters.

1. Introduction

Noble metal nanoparticles are characterized by unique optical properties, so called localized surface-plasmon resonances (LSPRs), with potential applications in biology sensing[1], cancer therapy[2], optoelectronic devices, photocatalysis and photovoltaics[3], etc. LSPRs are collective excitations of the conduction electrons that cause a strong absorption band in the UV-visible domain in the case of coinage metals. The LSPR frequencies can be tuned through the shape, size and composition of the nanoparticles[4,5]. For silver, the plasmon-like behavior is visible down to small cluster sizes of about 18-20 atoms[6].

While the LSPR is an intrinsic property of the metal cluster and could be investigated in gas phase[7], the experimental photoabsorption studies are frequently carried out on clusters in interaction with their environment, i.e. in solution[8] or in solid matrix[9], in order to control the stability and obtain a high density. These interactions are complex and poorly understood while they may have important effects on the optical response. Several transparent matrix materials such as photosensitive glass[10], alumina[11], silica[12,13] and Si_3N_4 [14] has been reported over a wide size range from few nm to a few hundred nm of diameter. Silver nanoparticles and nanoclusters have also been embedded in rare-gas matrices at low temperature[15-19]. Though the rare-gas matrices are relatively inert, and are more appropriate to characterize the intrinsic properties of clusters, some matrix effects on spectra are expected. They can be rationalized in two main competing effects[20]: the dielectric screening for the electron–electron interaction involves a redshift of the plasmon frequency as the dielectric constant of the matrix increases[21], while a confinement of the valence electrons of the cluster due to the presence of the rare-gas atoms may lead to a blue-shift for small clusters[22]. A more detailed discussion about the matrix effects can be found in Ref [20]. As both dielectric effects and confinement effects is expected to be size-dependent, the shift of the LSPR absorption band may present a size-dependent character. However in the case of Ag_n clusters with n=2-39, Fedrigo et al[16,17] have observed that the energy shift caused by changing the matrix gas is relatively independent of the cluster size, they measured a redshift of 0.22 eV (Ar →Xe) and 0.13 eV (Kr → Xe) for clusters of n=7-21 atoms. Based on the classical Mie approach with a two-domain dielectric function describing a spherical particle embedded in a medium, they have calculated that the plasmon-like band in silver clusters was likely to be red shifted by 0.24 / 0.32 / 0.42 eV when the clusters are embedded in an argon/krypton/xenon matrix with respect to the gas phase, in correct agreement with their experimental data. They concluded that changing the matrix gas Ar→Kr→Xe induces a redshift which is comparable for all sizes studied and does not affect the main

structure of the absorption spectra. To compare measurements made using different matrices, or to obtain the corresponding resonance energies in vacuum, the experimental data are often simply shifted by a constant value, estimated from the dielectric constants, for example plasmon bands measured in argon was shifted by 0.24 eV [17] or 0.29 eV [4].

Optical absorption spectra for silver clusters embedded in helium nanodroplets[23-25] and argon nanodroplets[26] have been reported too. Particularly, the optical spectra of rare gas-doped silver clusters in a helium droplet, $Ag_8RG_N@He_{droplet}$, have showed that the doping with RG=Ar, Kr, Xe leads to a shift of the mean resonance position which depends on the nature and the number *N* of attached atoms[24]. However, in all cases the shift with respect to free Ag_8 is inferior to 0.1 eV. So the medium's effect is lower when the cluster is embedded in a droplet that it is when the cluster is inside a solid matrix, in agreement with the fact that a larger dielectric constant is measured for a matrix than for a droplet[24].

The calculation of photoabsorption spectra for intermediate-size metal clusters can nowadays be performed in the framework of the Time-Dependent Density Functional Theory (TDDFT),[27] provided that an appropriate density functional is used[28-30]. For silver clusters, the description of excited states requires a correction of the self-interaction error (SIE) [31], and a correct asymptotic behavior[30]. The best results have been obtained with range separated hybrid functionals which resolve a significant part of the self-interaction-error (SIE) problems and also improve the asymptotic behavior at long range thanks to the inclusion of the Hartree-Fock exchange[32]. However having good predictions on metal clusters containing more than few thousand of electrons is still challenging. As an explicit treatment of both s- and d-electrons is required for noble metal clusters, simulations on a system of more than few hundred atom is only possible using geometrical structures of high symmetry.

In the past few years, a great work has been dedicated to the study of electronic, magnetic and optical properties of bare silver clusters[28-33] without taking account their environment. Simulations taking into account the matrix effects remain challenging even for small-size clusters. To our knowledge, only few papers have considered noble metals surrounded by rare gas. The weak interactions of rare gas atoms with small silver clusters (Ag_n, n=2-8) and their effects on the optical spectra have been evaluated at TDDFT level through an explicit treatment of few surrounding rare gas atoms[34,35]. The matrix effects of a rare-gas matrix on the spectra of small silver clusters (Ag_n, n = 2, 4, 6, 8, 20), were estimated using an electrostatic model of solvation (the conductor-like screening model of solvation (COSMO) model) in TDDFT/GGA calculations[36]. Compared to the gas phase, an average red-shift of 0.17, 0.20, and 0.26 eV of the main peaks in argon, krypton, and xenon matrices respectively were

obtained. The average shift was calculated at 0.06 eV for Xe → Kr and 0.09 eV for Xe → Ar, underestimating the experimental values of 0.13 and 0.22 eV respectively[17]. More reliable results would need to adopt a more refined embedding model[22], or to explicitly include rare gas atoms in the calculations. Very recently, Xuan and Guet[37] have studied the environment effect induced by a rare-gas matrix on silver Ag_n clusters with closed shell number of electrons (n = 8, 20, 58, 92, 138, 198) within a modified random phase approximation with exact exchange quantum approach. The model, which not considers explicitly the geometrical structure, treats the polarization by the embedding rare-gas medium and that by the silver core on equal footing using an appropriate core-polarization term. A significant red shift of the oscillator strength peak was found due to matrix screening on the dipole term of the two-body Coulomb interaction.

Here we investigate the absorption spectra of silver clusters embedded in a rare gas matrix. We present a methodology in which the metal clusters is surrounded by explicit rare-gas atoms and embedded in a polarizable continuum medium. Optical response is calculated in the TDDFT approach. The present paper is organized as follows: In Section 2, we describe our theoretical approach which aims to mimic the experimental conditions where preformed metal clusters are embedded inside an amorphous rare-gas matrix[6,15-19], then in Section 3 our results are discussed and compared to available experimental data.

2. Computational method

In our DFT and TDDFT calculations we explicitly include 100 rare gas atoms around the silver cluster, and the Ag_nRG_{100} cluster is placed inside a cavity surrounded by a dielectric medium described by a dielectric function through a polarizable continuum model (PCM).[38] In details, calculations have been performed as follows. First we optimize the structure of the cluster Ag_nRG_{100} placed in a dielectric medium characterized by the dielectric function of the solid rare gas RG = Ne, Ar, Kr, or Xe. The dielectric constants, $\varepsilon_{Ne} = 1.5$, $\varepsilon_{Ar} = 1.7$, $\varepsilon_{Kr} = 1.9$, and $\varepsilon_{Xe} = 2.22$ were taken from Ref [39], they are very similar to the values used in previous investigations[17,24,36,37]. In Figure 1, we show the dependence on the dielectric constant of the absorption spectrum for Ag_{20} embedded in neon matrix. As expected the plasmon-like band is red shifted with increasing ε. The band that is centered at 3.97 eV in gas phase, shifts to 3.95, 3.86, 3.80, 3.75, and 3.70 eV for $\varepsilon_{Ne} = 1.1, 1.3, 1.5, 1.7, 1.9$ respectively. The value of 1.5 leads to a very good agreement with the experimental data of 3.83 eV [19]. Another effect of

the matrix is the broadening of the band which is relatively independent of the ε_{Ne} value. Some details on the treatment of the silver-neon interface are given in Supporting Information. Using 100 Ne buffer atoms allows us to form a fully complete shell surrounding Ag_{92}. Figure S1 (Supporting Information) shows that a single complete shell is required and sufficient to correctly describe the interface.

The geometrical structures of Ag_{35}, Ag_{58} and Ag_{92} were taken from a study by Chen et al[40] dedicated to the prediction of structures of silver clusters using a genetic algorithm with an embedded atom method potential, while the structure of Ag_{20} is the ground state structure of C_s symmetry optimized at DFT level in Ref [6]. Of course we cannot be sure that a more stable cluster than those considered in our calculations does not exist, but our tests show that the spectra characterized by a plasmon-like band are only weakly dependent on the exact geometrical structure as long as the shape is somewhat spherical. The initial position of rare-gas atoms around the metal cluster was generated by a homemade program in order to obtain an amorphous arrangement. Then the structure of Ag_nRG_{100} was optimized using the ωB97xD functional[41] which includes 100% exchange Hartree-Fock at long range and an empirical dispersion term. Finally TDDFT absorption spectra are calculated with the hybrid functional ωB97x[42] within the solvent reaction field.

We think that the methodology is suitable to describe the experimental protocol where preformed and size-selected Ag_n clusters are codeposited with rare gas atoms at low-energy on a window cooled at few kelvin (~5-10K), resulting into an amorphous rare gas matrix in which metal clusters are embedded [6,16,17].

All calculations were performed with the Gaussian09 suite of programs[43]. Pre- and postprocessing operations were performed by using the graphical interface Gabedit[44]. For silver, a relativistic effective core potential (RECP) was used, so that only 19 valence electrons per atom were treated explicitly, together with the corresponding Gaussian basis set[45]. For Ne and Ar atoms, we use the 6-311++G basis set from the G09 basis set library. For Kr and Xe, we used a RECP together with the corresponding basis set[45] to which we added a s and p type diffuse function (coefficients 0.06 and 0.07 for Kr, 0.04 for Xe). However very similar spectra have been obtained using the 6-311++G basis set. Spectra presented in the figures are plotted with a Lorentzian broadening (fwhm = 0.08 eV).

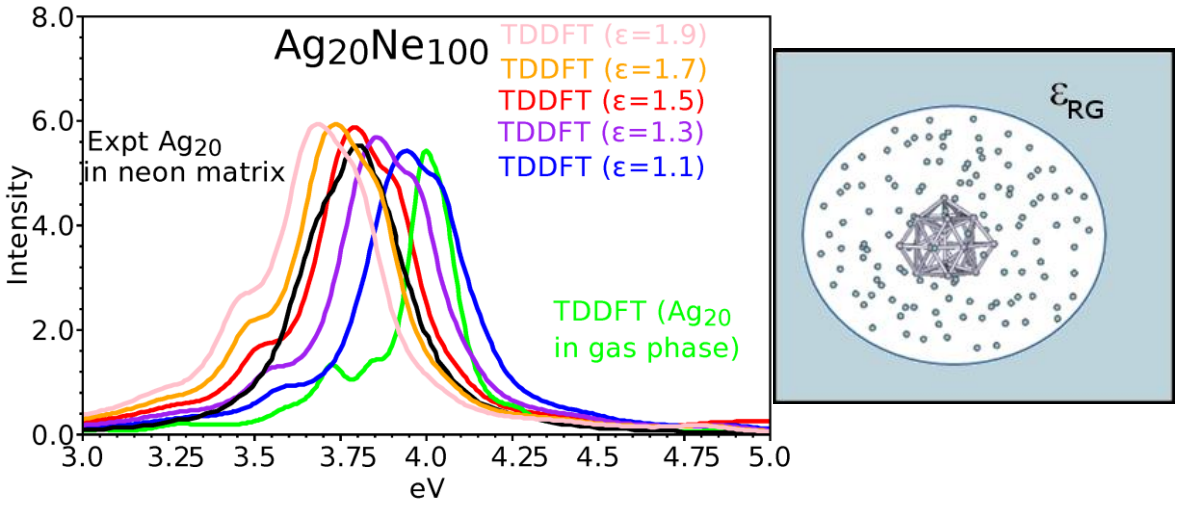

Figure 1. Absorption spectrum of Ag_{20} in a neon matrix calculated with several dielectric constants (1.1 – 1.9) together with the spectrum calculated in the gas phase (green line) and the experimental spectrum in neon matrix[19] (black line). On the right, a scheme of the model showing Ag_{20} surrounded by 100 rare-gas (RG) atoms while the effects of the more distant atoms are modeled via a dielectric medium characterized by the dielectric function ε_{RG}.

3. Results and Discussion

3.1 Ag_{20} in rare-gas matrix

Our calculated absorption spectra for Ag_{20} embedded in Ne, Ar, Kr, and Xe matrices are given in Figure 2. For Ne and Ar matrices, we also show the experimental spectrum[6,19]. To our knowledge, no experimental data are available for Ag_{20} in Kr and Xe matrices. However, we give in Figure 2, in dashed curves, the spectrum of Ag_{21} that were measured by Fedrigo et al.[17]. Spectra of Ag_{20} and Ag_{21} measured in Ar were found to be very similar[6], and we think that it should be the same in Kr and Xe matrices. Figure 2 shows that our results are clearly in very good agreement with the experiment. For Ag_{20} in Ne, the experimental band is centered at 3.83 eV and was fitted by three Gaussian functions at 3.68, 3.79 and 3.87 eV [19]. In our calculation, several peaks scattered in the 3.7-3.83 eV range leads to a central band at 3.81 eV, with a shoulder at 3.92 eV and a smaller peak at 3.51 eV. The calculated spectrum for Ag_{20} in Ar present several peaks between 3.66 and 3.83 eV, followed by a large intensity peak at 3.87 eV. The agreement with the experiment is also good but the shoulder at 4 eV is not reproduced, it could correspond to the calculated transition at 3.87 eV. Spectra for Ag_{20} in Kr and Xe present

a large band made of several peaks well scattered between 3.3 and 3.8 eV, the band extends at low energies down to 3 eV. They are somewhat similar to the experimental spectra of Ag_{21} although the band is slightly wider.

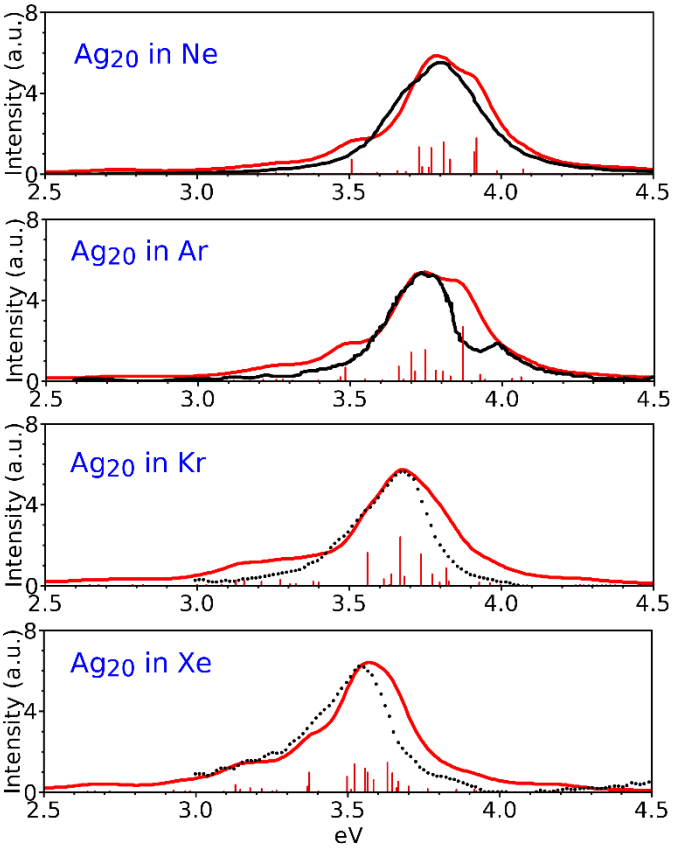

Figure 2. Calculated absorption spectra (in red) of Ag_{20} in Ne, Ar, Kr and Xe matrices compared to the experimental spectrum of Ag_{20} in Ne and Ar (black line) [6,19] and that of Ag_{21} in Kr and Xe (dashed curve) [17].

The plasmon band of Ag_{20}, centered at 3.97 eV in phase gas, shifts to 3.80, 3.76, 3.66, and 3.56 eV for Ne, Ar, Kr, Xe matrices respectively. Hence we calculated a red shift by changing the matrix gas of 0.2 eV (Ar → Xe), 0.1 eV (Kr→ Xe) and 0.1 eV (Ar → Kr). These values are in good agreement with the experimental shifts measured[17] at 0.22 eV (Ar →Xe), 0.13 eV (Kr → Xe), 0.09 eV ((Ar → Kr). The good agreement between our predictions and the experimental data clearly validates our results and our methodological approach.

In our methodology, we chose to place explicitly 100 rare gas atoms between the metal cluster and the area described by the continuum media. In Figure 3, we show the need to treat explicitly a layer of rare gas atoms. When the metal is placed directly in contact with the

continuum media described the dielectric constant, the plasmon band becomes strongly broadened and asymmetric. The presence of the continuum medium in contact to silver atoms leads to an inhomogeneous fragmentation of the plasmon. Explicit rare gas atoms around the metal cluster serve as a buffer zone and their presence reduces the unexpected effects.

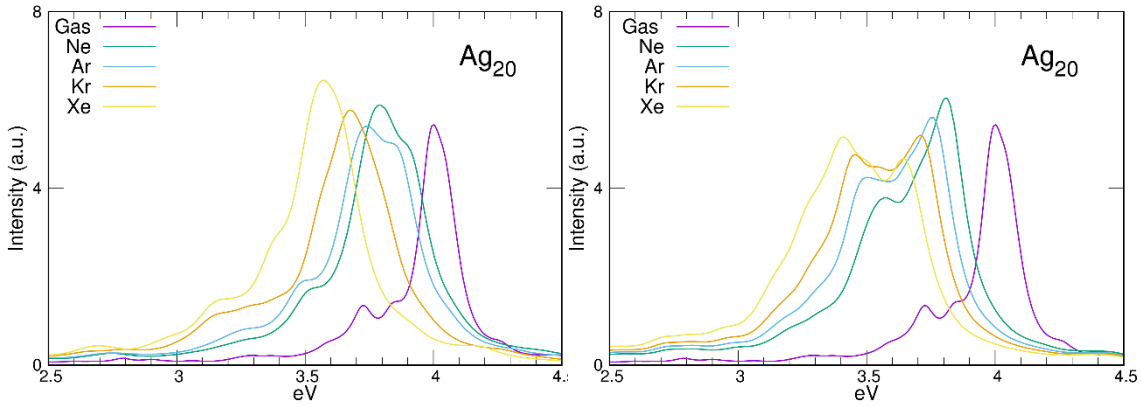

Figure 3. Calculated absorption spectra of Ag_{20} in gas phase or in Ne, Ar, Kr and Xe matrix. a) Left: Spectra calculated with 100 rare gas atoms explicitly around the metal cluster, b) Right: Spectra calculated for Ag_{20} directly in the dielectric medium without explicit rare gas atoms.

3.2 Ag_n in Ne matrix

We have simulated the absorption spectra of larger clusters in a neon matrix for which experimental data have recently been published[19]. The other matrices have not been considered because of lack of experimental results and also the high cost of calculation. In figure 4 we give our results for $Ag_{35,58,92}$ surrounding by 100 Ne atoms and the polarizable continuum medium. The plasmon band is calculated to be centered at 3.79, 3.95, and 3.85 eV for Ag_{35}, Ag_{58}, Ag_{92} respectively, in good agreement with the experimental data of 3.84, 3.93, 3.80 eV [19]. For Ag_{35}, the spectrum presents a relative wide band, composed of two humps calculated at 3.68 and 3.82 eV respectively, and a shoulder at 3.93 eV followed by a smaller intensity peak at 4.22 eV. The band fits well the experimental spectrum which presents two humps at 3.70 and 3.94 eV respectively. For $Ag_{58,}$ the calculated spectrum is composed of a broad absorption band due to a strong dispersion of the oscillator strengths over the 3.5-4.5 eV energy range with no dominant peak. The calculated band is in good agreement with the experimental one, which presents a main peak at 3.94 eV and a shoulder at 3.64 eV [19], even if the shape of the band is not exactly

reproduced. The calculated spectrum of Ag_{92} is very similar to the experimental one despite a shift of 0.05 eV. In particular, the narrow width is well reproduced and could be interpreted as a signature of a symmetrical structure, like the C_{3v}-symmetry structure used in our calculation. The calculated plasmon band is centered at 3.86 eV.

Compared to the spectrum calculated in gas phase, the red shift induced by the Ne matrix effects is relatively independent on the cluster size n in the range of n = 20 - 92. In a recent paper[19], we have evaluated the red shift at 0.17 eV. In the present study, we have estimated the red shift for sizes n = 20, 35, 58, 92 with several configurations miming the Ne matrix. In all calculations, the red shift ranges between 0.14 and 0.19 eV, with a mean value close to 0.17 eV. Using the density functional ωB97x and the basis set LanL2DZ[45] on silver atoms for calculations in gas phase and in matrix, we have calculated a redshift of 0.17, 0.14, 0.17, and 0.19 eV for n = 20, 35, 58, and 92 respectively. It is clear that the dielectric effects, responsible for the redshift, overcome the effects of confinement which, on the contrary, should lead to a blue shift. It is true at least until the small size of 20 atoms.

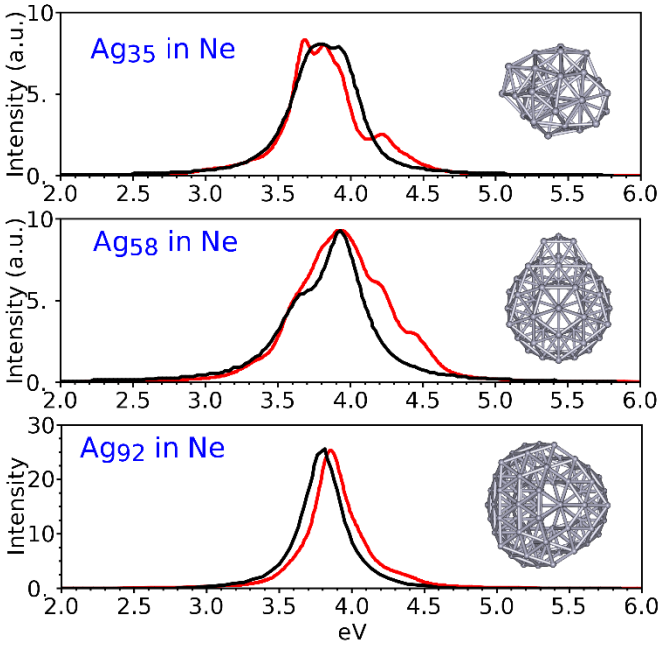

Figure 4. Calculated absorption spectra (red curve) of $Ag_{35,58,92}$ in a neon matrix compared to the experimental spectrum (black curve) taken from [19]. Structures of bare clusters are also depicted.

We have also studied a smaller cluster, Ag_8, embedded in the Ne matrix in order to know if the red shift is still valid at very small size. The absorption spectrum of Ag_8 in Ne matrix

have been measured by Lecoultre et al.[18], we plot it in Figure 5. It is composed of two intense transitions at 3.65 and 4.00 eV, and two small narrow peaks at 3.12 and 3.20 eV. It is now well known that two structures of symmetry D_{2d} and T_d (see Figure 5) compete for the lowest-energy isomer. The energy ordering is dependent of the density functional used[18,20,46], while at CCSD(T) level the T_d structure was predicted to be more stable within 0.03 eV [40]. Using the ωB97x functional, the T_d structure is also favored. Spectra for both structures are given in Figure 5. For Ag_8 (T_d) in Ne matrix, the calculation predicts an intense 3-fold degenerate peaks at 4.08 eV, and a second one at 3.18 eV. For Ag_8 (D_{2d}) in Ne matrix, the main transition is a doubly degenerate peak at 4.02 eV and a peak at 3.64 eV. Three experimental transitions (at 3.12, 3.20, and 4.00 eV) could correspond to transitions calculated for the T_d isomer (3.18 and 4.08 eV), while two experimental peaks at 3.65 and 4.00 eV are well reproduced by transitions calculated for the D_{2d} isomer at 3.64 and 4.02 eV. As previously suggested,[6,20] both isomers could be present in the experiment, the experimental spectrum being then a sum of the spectra for both isomers. Interestingly, we compare in Figure 5 the absorption spectrum of Ag_8 calculated in Ne matrix and in gas phase. For the T_d structure, spectra are nearly similar since the peaks are found at 3.22 and 4.05 eV in gas phase (compared to 3.18 and 4.08 in Ne matrix). So, the confinement effect overcomes dielectric effects resulting in a small blue shift of 0.03 eV for the main band. For the D_{2d} structure, the peaks in gas phase are calculated to be at 3.74 and 4.00 eV respectively, compared to 3.64 and 4.02 eV in Ne matrix. The matrix affects differently the two peaks: the doubly degenerate peak near 4 eV is slightly blue shifted (by 0.02 V), while the other is red shift by 0.1 eV. Actually these peaks come from the fragmentation of a unique 3-fold degenerate transition in a spherical nanoparticle and associated to a plasmon-like resonance. The degeneracy can still be observed in the T_d structure (transition at 4.08 V), but not in the D_{2d} due to a spatial symmetry breaking and a lift of the degeneracy. If we consider the transitions at 3.74 and 4.00 eV of the D_{2d} structure as a fragmented plasmon-like band, we obtained an average position of 3.89 eV by integrating the peaks, this average position is red shifted to 3.84 eV in Ne matrix. We plot in Figure 6 the induced density for the peaks at 3.74 and 4.00 eV. The former corresponds to an excitation along the longitudinal axis (z-direction) of the D_{2d} structure, while the latter corresponds to a motion along the short axis (x- and y-direction). Electron motions are much more affected by the confinement when oscillations happen in transverse directions than in the longitudinal mode. Based on the atomic structure, one can model the cluster by a box with a long side of 4.5 Å and two short sides of 3.7 Å. An additional confinement due to the presence of the Ne atoms will have a greater impact for motions along the short axis. Consequently, the confinement effect is large enough to balance

the dielectric effect and cancel the red shift for transverse modes (peak at 4.0 eV). On the contrary, for the longitudinal mode, the confinement is smaller, and the dielectric effects dominate resulting in a red shift of 0.1 eV. Then one can estimate that for clusters with a diameter > 4.5 Å (about 12-15 atoms), the matrix effects are mainly of dielectric nature and lead to a red shift. Also, it has been showed that calculations for Ag_n in gas phase, with n=4-12, reproduce well the experimental data measured for clusters embedded in matrix[28]. That is also in line with the confinement effects roughly balancing the dielectric effects for $n \leq 12$.

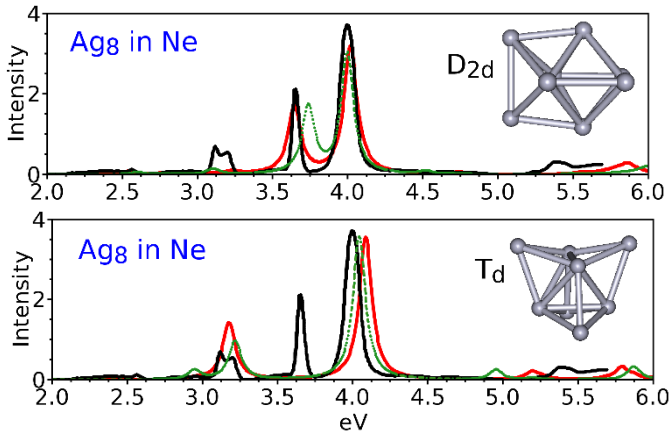

Figure 5. Calculated absorption spectra of Ag_8 in a neon matrix (red curve) compared to the experimental spectrum (black curve) taken from [18]. Calculated spectra of Ag_8 in gas phase are given in green dashed curve. D_{2d} and T_d symmetry structures of bare clusters are also depicted.

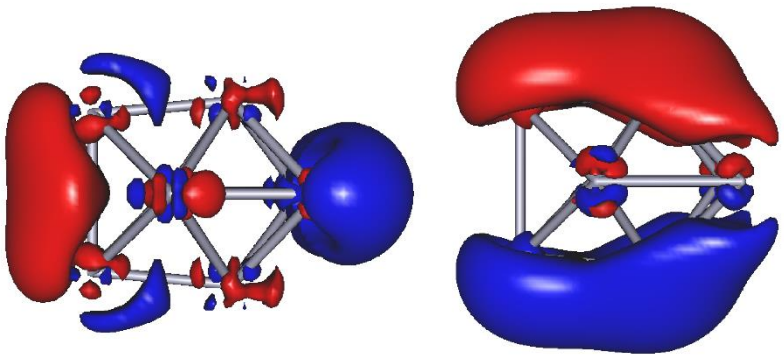

Figure 6. Plots of the induced density calculated for the peaks at 3.74 (left, longitudinal mode) and 4.00 eV (transverse modes) for the D_{2h} structure of Ag_8 in the gas phase.

4. Conclusions

The optical response of silver clusters embedded in a rare-gas (Ne, Ar, Kr, Xe) matrix have been calculated in the framework of the TDDFT. In our approach, the metal cluster was surrounded by explicit rare-gas atoms and embedded in a polarizable continuum medium. Interactions with the surrounding medium affects both the position and the width of the surface plasmon absorption band of metal clusters. The size dependent shift of the plasmon band have been studied in the case of a neon matrix. Our results have showed that for n = 20 – 92 the dielectric effects overcome the confinement, resulting in a redshift of about 0.17 eV without a significant size dependency, but the confinement effects balance the dielectric effects for small cluster (n = 8, and expected up to n ≅ 12) and cancel the redshift. Our results reproduce the experimental spectra with unprecedented accuracy.

Acknowledgement

Present work has received a financial support from the French National Research Agency (Agence Nationale de la Recherche, ANR) in the frame of the project “FIT SPRINGS”, ANR-14-CE08-0009. The authors thanks the Pôle Scientifique de Modélisation Numérique (PSMN) at Lyon, France, and the GENCI-IDRIS (Grant i2016086864) center for generous allocation of computational time. The authors gratefully acknowledge W. Harbich and J. Lermé for helpful discussions.

References

[1] Anker, J. N.; Paige-Hall, W.; Lyandres, O.; Shah, N. C.; Zhao, J.; Van-Duyne, R. P. Biosensing with plasmonic nanosensors. *Nat. Mater.* **2008**, 7, 442−453.

[2] Bardhan, R.; Lal, S.; Joshi, A.; Halas, N. J. Theranostic nanoshells: from probe design to imaging and treatment of cancer. *Acc. Chem. Res.* **2011**, 44, 936−946.

[3] Chen, Y.-S.; Choi, H.; Kamat, P. V. Metal-Cluster-Sensitized Solar Cells. A new class of thiolated gold sensitizers delivering efficiency greater than 2%. *J. Am. Chem. Soc.* **2013**, 135, 8822-8825.

[4] Haberland H. Looking from both sides. *Nature* **2013**, 494, E1-E2.

[5] Sinha-Roy, R.; Garcia-Gonzalez, P.; Weissker, H.-C.; Rabilloud, F.; Fernandez-Dominguez, A.I. Classical and ab initio plasmonics meet at sub-nanometric noble metal rods. *ACS Photonics* 2017, 4, 1484-1493.

[6] Harb, M. ; Rabilloud, F. ; Simon, D. ; Rydlo, A. ; Lecoultre, S. ; Conus, F. ; Rodrigues, V. ; Félix, C. Optical absorption of small silver clusters : Ag_n, (n=4-22). *J. Chem. Phys*, **2008**, 129, 194108.

[7] Tiggesbäumker, J.; Köller, L.; Meiwes-Broer, K.-H.; Liebsch A. Blue shift of the Mie plasma frequency in Ag Clusters and particles. *Phys. Rev. A* **1993**, 48, R1749-R1752.

[8] Cure, J.; Coppel, Y.; Dammak, T. ; Fazzini, P. F. ; Mlayah a. ; Chaudret, B. Fau, P. Monitoring the coordination of amine ligands on silver nanoparticles using NMR and SERS. *Langmuir* **2015**, 31, 1362-1367.

[9] Cottancin, E.; Lermé, J.; Gaudry, M.; Pellarin, M.; Vialle, J.-L.; Broyer, M.; Prével, B.; Treilleux, M.; Mélinon P. Size effects in the optical properties of Au_nAg_n embedded clusters. *Phys. Rev. B* **2000**, 62, 5179-5185.

[10] Genzel, L.; Martin, T. P.; Kreibig, U. Dielectric function and plasma resonances of small metal particles. *Z. Phys. B*, **1975**, 21, 339–46.

[11] Cottancin, E.; Celep, G.; Lermé, J.; Pellarin, M.; Huntzinger, J. R.; Vialle, J. L.; Broyer, M. Optical properties of noble metal clusters as a function of the size: comparison between experiments and a semi-quantal theory. *Theor. Chem. Acc.* **2006**, 116, 514-523.

[12] Hilger, A.; Cüppers, N.; Tenfelde, M.; Kreibig, U. Surface and interface effects in the optical properties of silver nanoparticles. *Eur. Phys. J. D* **2000**, 10, 115–118.

[13] Hillenkamp, M.; Di Domenicantonio, G.; Eugster, O.; Félix, C. Instability of Ag nanoparticles in SiO_2 at ambient conditions. *Nanotech*. **2007**, 18, 015702.

[14] Raza, S.; Kadkhodazadeh, S.; Christensen, T.; Di Vece, M.; Wubs, M.; Mortensen, N. A.; Stenger, N. Multipole plasmons and their disappearance in few-nanometer silver nanoparticles. *Nat. Commun.* **2015**, 6, 8788.

[15] Charlé, K.-P.; Schulze W.; Winter, B. The size dependent shift of the surface plasmon absorption band of small spherical metal particles. *Z. Phys. D – At., Mol. Clust.* **1989**, 12, 471-475.

[16] Harbich, W.; Fedrigo, S.; Buttet, J. The optical absorption spectra of small Silver clusters (n=8-39) embedded in rare gas matrices. *Z. Phys. D – At., Mol. Clust.* **1993**, 26, 138-140.

[17] Fedrigo, S.; Harbich, W.; Buttet, J. Collective dipole oscillations in small silver clusters embedded in rare-gas matrices. *Phys. Rev. B* **1993**, 47, 10706-10715.

[18] Lecoultre S.; Rydlo, A.; Buttet, J.; Félix, C.; Gilb, S.; Harbich, W. Ultraviolet-visible absorption of small silver clusters in neon: Ag_n, (n=1-9). *J. Chem. Phys*, **2011**, 134, 184504.

[19] Yu, C.; Schira, R.; Brune, H.; von Issendorf, B.; Rabilloud, F.; Harbich, W. Optical properties of size selected neutral Ag clusters: electronic shell structures and the surface plasmon resonance. *Nanoscale, accepted.* *http://dx.doi.org/10.1039/C8NR04861D*

[20] Anak, B.; Bencharif, M.; Rabilloud, F. Time-dependent density functional study of UV-visible absorption spectra of small noble metal clusters (Cu_n, Ag_n, Au_n, n=2-9, 20). *RSC Advances* **2014**, 4, 13001-13010.

[21] Rubio, A.; Serra, L. Dielectric screening effects on the photoabsorption cross section of embedded metallic clusters. *Phys. Rev. B: Condens. Matter* **1993**, 48, 18222–18229.

[22] Gervais, B.; Giglio, E.; Jacquet, E.; Ipatov, A.; Reinhard, P.-G.; Fehrer, F.; Suraud, E. Spectroscopic properties of Na clusters embedded in a rare-gas matrix. *Phys. Rev. A* **2005**, 71, 015201-015210.

[23] Federmann, F.; Hoffmann, K.; Quaas, N.; Toennies J. P. Spectroscopy of extremely cold silver clusters in helium droplets. *Eur. Phys. J. D.* **1999**, 9, 11-14.

[24] Diederich, T.; Tiggesbäumker, J.; Meiwes-Broer K.-H. Spectroscopy on rare gas-doped silver clusters in helium droplets. *J. Chem. Phys.* **2002**, 116, 3263-3269.

[25] Loginov, E.; Gomez, L. F.; Chiang, N.; Halder, A.; Guggemos, N.; Kresin, V. V.; Vilesov A. F. Photoabsorption of Ag_N (N ~ 6–6000) nanoclusters formed in helium droplets: transition from compact to multicenter aggregation. *Phys. Rev. Lett.* **2011**, 106, 233401.

[26] Christen, W; Radcliffe, P.; Przystawik, A.; Diederich, Th.; Tiggesbäumker, J. Argon solvent effects on optical properties of silver metal clusters. *J. Phys. Chem. A* **2011**, 115, 8779-8782.

[27] Casida, M. E. In Recent Advances in Density-Functional Methods; Chong, D. P., Ed.; World Scientific: Singapore, 1995; p 155.

[28] Rabilloud, F. Assessment of the performance of long-range-corrected density functionals for calculating the absorption spectra of silver clusters. *J. Phys. Chem. A* **2013**, 117, 4267-4278.

[29] Rabilloud, F. UV-visible absorption spectra of metallic clusters from TDDFT calculations. *Eur. Phys. J. D* **2013**, 67, 18.

[30] Baseggio, O.; De Vetta, M.; Fronzoni, G.; Mauro Stener, M.; Sementa L.; Fortunelli, A.; Calzolari A. Photoabsorption of icosahedral noble metal clusters: an efficient TDDFT approach to large-scale systems. *J. Phys. Chem. C* **2016**, 120, 12773-12782.

[31] Rossi, T. P.; Kuisma, M.; Puska, M. J.; Nieminen, R. M.; Erhart, P. Kohn–Sham decomposition in real-time time-dependent density-functional theory: an efficient tool for analyzing plasmonic excitations. *J. Chem. Theory Comput.* **2017**, 13, 4779−4790.

[32] Rabilloud, F. Description of plasmon-like band in silver clusters: the importance of the long-range Hartree-Fock exchange in time-dependent density-functional theory simulations. *J. Chem. Phys.* **2014**, 141, 144302.

[33] Koval, P.; Marchesin, F.; Foerster, D.; Sánchez-Portal, D. Optical response of silver clusters and their hollow shells from linear-response TDDFT. *J. Phys.: Condens. Matter* **2016**, 28, 214001.

[34] Yasrebi S.; Jamshidi Z. Theoretical investigation of the weak interactions of rare gas atoms with silver clusters by resonance Raman spectroscopy modeling. *Int. J. Quantum Chem.* **2017**, 117, 1-9.

[35] Pereiro, M.; Baldomir, D.; Arias, E. A first-principles study of the influence of helium atoms on the optical response of small silver clusters. *J. Chem. Phys.* **2011**, 134, 084307.

[36] Jensen, L.; Zhao, L. L.; Schatz G. C. Size-dependence of the enhanced Raman scattering of pyridine adsorbed on Ag_n (n = 2-8, 20) clusters. *J. Phys. Chem. C* **2007**, 111, 4756-4764.

[37] Xuan, F.; Guet, C. Medium-induced change of the optical response of metal clusters in rare-gas matrices. *Phys. Rev. A* **2017**, 96, 043404.

[38] Tomasi, J.; Mennucci, B.; Cammi, R. Quantum mechanical continuum solvation models. *Chem. Rev.* **2005**, 105, 2999-3093.

[39] Kreibig U.; Vollmer, M. Optical properties of metal clusters, Springer Series in Materials Science Edition (Springer, Berlin, 1995), Vol. 25.

[40] Chen, M.; Dyer, J. E.; Li K.; Dixon, D. A. Prediction of structures and atomization energies of small silver clusters Ag_n, n<100. *J. Phys. Chem. A* **2013**, 117, 8298-8313.

[41] Chai J.-D.; Head-Gordon, M. Long-range corrected hybrid density functionals with damped atom-atom dispersion corrections. *Phys. Chem. Chem. Phys.* **2008**, 10, 6615-20.

[42] Chai, J.-D.; Head-Gordon, M. Systematic optimization of long-range corrected hybrid density functionals. *J. Chem. Phys.* **2008**, 128, 084106

[43] Frisch M.J. et al. *Gaussian09*, Revision D.01, Gaussian Inc., Wallingford CT, 2013.

[44] Allouche, A. R. Gabedit A Graphical user interface for computational chemistry softwares. J. Comput. Chem. 2011, 32, 174−182.

[45] Hay P. J.; Wadt, W. R. *Ab initio* effective core potentials for molecular calculations. Potentials for K to Au including the outermost core orbitals. *J. Chem. Phys.* **1985**, 82, 299.

[46] Die, D.; Shen, X.-Y.; Song, C.-Y.; Du, Q. The puzzling optical-absorption and photoelectron spectra of neutral and anionic Ag_8 clusters. *Spectrochimica Acta Part A: Molecular and Biomolecular Spectroscopy* **2019**, 206, 535.

TOC

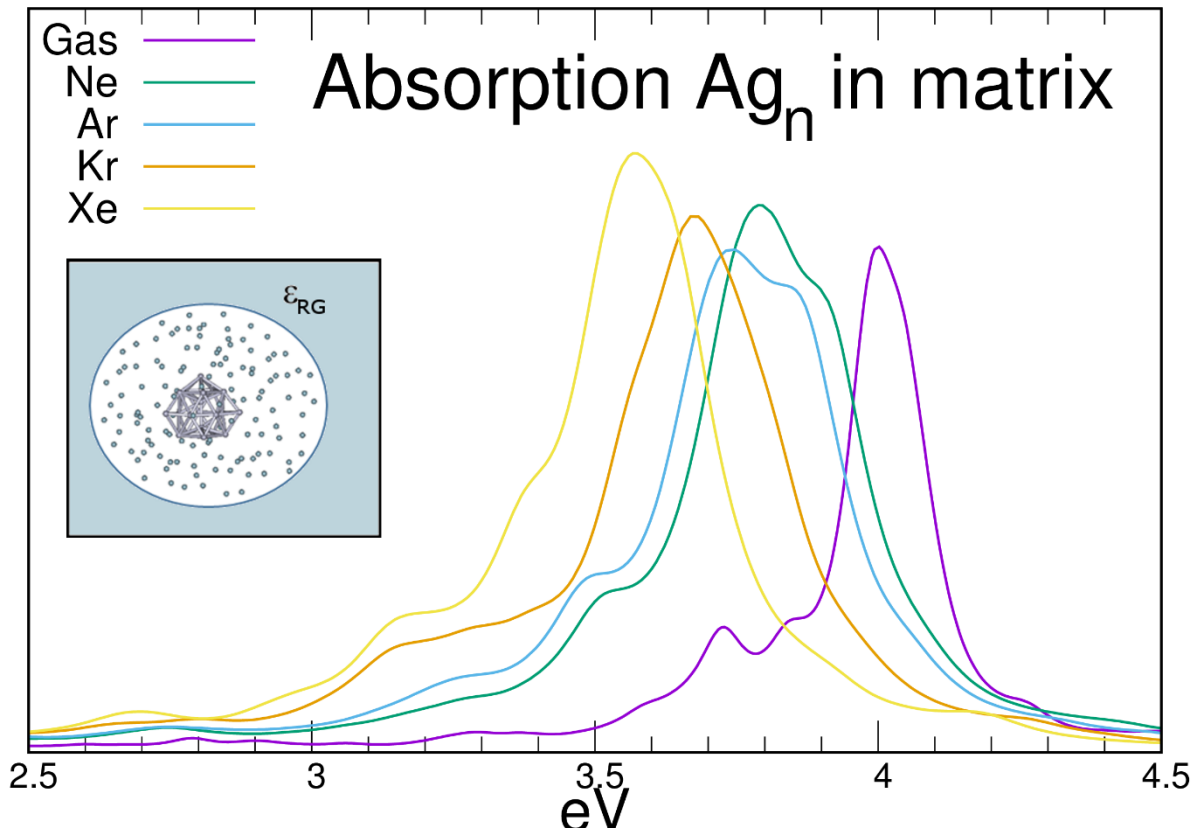
Gas
Ne
Ar
Kr
Xe
Absorption Ag$_n$ in matrix
ε_{RG}
2.5
3
3.5
4
4.5
eV